


Cite this: *RSC Adv.*, 2021, **11**, 22131

# Investigation of anti-aging of SBS modified bitumen containing surface organic layered double hydroxide

Canlin Zhang,<sup>abc</sup> Hongjun Dong,<sup>ab</sup> Ting Wang,<sup>\*d</sup> Song Xu,<sup>\*ab</sup> Jun He,<sup>ab</sup> Lei Fang<sup>ab</sup> and Changbin Hu<sup>ab</sup>

To improve the anti-aging ability of SBS modified bitumen (SMB), layered double hydroxide (LDH) organically modified by hexadecyltrimethoxysilane was prepared and utilized for the modification of SMB. According to X-ray photoelectron spectroscopy, hexadecyltrimethoxysilane has been grafted into LDH through chemical bonding. Compared with LDH, the hydrophilicity of organic LDH (OLDH) was obviously reduced, and OLDH possessed better dispersibility and stability in SMB, because of the decrease of hydroxyl and the introduced organo-functional groups on the surface of LDH. The addition of OLDH and LDH can ameliorate the high temperature behavior of SMB, especially OLDH. After aging, bitumen was oxidized and SBS was degraded, which resulted in the physical and rheological property deterioration of SMB. LDH can alleviate the destruction of aging on the performance and chemical structure of SMB. Furthermore, the improvement of LDH on the anti-aging ability of SMB has been further enhanced after hexadecyltrimethoxysilane organic modification.

Received 24th May 2021  
Accepted 12th June 2021

DOI: 10.1039/d1ra04042a

rsc.li/rsc-advances

## 1. Introduction

SBS modified bitumen (SMB) has been become the uppermost binding material in highway construction, because of its excellent high-temperature rutting resistance and low-temperature cracking resistance, which is due to the formed crosslinked network structure of SBS in bitumen.<sup>1–3</sup> Unfortunately, under the influence of heat, oxygen and UV light, SMB is liable to aging, which causes the performance degradation of SMB and ultimately shortens the service life of bitumen pavement.<sup>4–8</sup> Hence, it is essential to acquire SMB with superior anti-aging ability. In recent years, some antiaging agents have been utilized to improve the anti-aging ability of SMB, such as anti-oxidants, UV absorbents, inorganic nanoparticles, layered silicate, and so on.<sup>9–11</sup> These modifying agents can all improve the anti-aging ability of SMB to different extents, but there are some imperfections in these modifying agents, for instance, antioxidants can only improve the thermal oxidation aging resistance of SMB and the sustaining action is limited. The improvement effect of UV absorbents on the anti-aging is closely linked to the types of SMB.<sup>10,12</sup> The compatibility of inorganic nanoparticles

in SMB is poor.<sup>13,14</sup> Layered silicate is harmful to the low temperature property of SMB.<sup>9,12</sup> These deficiencies affect the improving effectiveness of these modifying agents on the anti-aging ability of SMB, and eventually restrict their application in SMB.

Layered double hydroxide (LDH) is a supramolecular material with multilayered structure, which is composed of metallic-oxide laminate and interlamellar anions.<sup>15,16</sup> The metallic-oxide laminate can shield UV light, and obstruct oxygen and heat. Simultaneously, the interlamellar anions can also assimilate UV light.<sup>17,18</sup> Therefore, LDH is considered as an ideal choice to ameliorate the anti-aging performance for bitumen, and it has been used as modifier for SMB in recent years, compared with unmodified SMB, SMB containing LDH exhibits better physical and rheological performance after aging.<sup>19,20</sup> However, some studies found that LDH can not uniformly disperse and stably exist in bitumen, this restricted the sufficient exertion of LDH on improving the anti-aging ability of bitumen. The reason for this is the hydroxide radical on the surface of LDH, the hydroxide radical will cause the conglomeration between LDH particles.<sup>18,21</sup> To settle the issue, some organic anion compounds were replaced into the interlamination of LDH, like lignosulfonate, salicylic acid, *p*-methycinnamic acid, etc.<sup>22–24</sup> Although intercalated LDH shows better effectiveness on the anti-aging performance of bitumen, unfortunately, the essential question (the hydroxide radical) of LDH has not been solved. Silane coupling agent is often used to heighten the compatibility between inorganic materials and organic materials.<sup>25</sup> Hence, silane coupling agent could be a perfect solution to the

<sup>a</sup>College of Civil Engineering, Fuzhou University, Fuzhou 350108, P. R. China. E-mail: xusong@fzu.edu.cn

<sup>b</sup>Fujian Provincial University Engineering Research Center for Advanced Civil Engineering Materials, Fuzhou University, Fuzhou 350108, P. R. China

<sup>c</sup>School of Advanced Manufacturing, Fuzhou University, Fuzhou 350108, P. R. China

<sup>d</sup>Testing Center of Fuzhou University, Fuzhou 350108, P. R. China. E-mail: wting@fzu.edu.cn



issue between LDH and SMB. On the one hand, the hydrolyzed hydroxyl of silane coupling agent would react with the surface hydroxyl of LDH, resulting in the surface hydroxyl decrease of LDH,<sup>26</sup> it is conducive to reduce the conglomeration between LDH particles, and enhance the dispersion of LDH in SMB. On the other hand, silane coupling agent will inlet organic groups into LDH, which is helpful for ameliorating the stability of LDH in hydrophobic SMB matrix.

In this research, silane coupling agent organic LDH (OLDH) was prepared and utilized to ameliorate the anti-aging capacity of SMB. The chemical structure and surface property of OLDH, and the influence of OLDH on the performance and structure of SMB before and after aging were studied.

## 2. Materials and methods

### 2.1. Materials

The 60/80 penetration-grade bitumen was acquired from CNOOC asphalt Co., Ltd. SBS was provided from Baling Branch of Sinopec Co., Ltd, the main performance parameters of bitumen and SBS are illustrated in Table 1. LDH (MgAl-CO<sub>3</sub>-LDH) was obtained from Ruifa Chemical Co. Ltd, hexadecyltrimethoxysilane was offered from Sinopharm Group Co. Ltd, the chemical structure diagram of LDH and hexadecyltrimethoxysilane are plotted in Fig. 1.

### 2.2. Preparation of OLDH

LDH was dispersed in ethanol–water solution (90%, volumetric fraction), and appropriate amount (3.5% by weight of LDH) of hexadecyltrimethoxysilane was added into the mixed solution. Under the nitrogen atmosphere, the reaction solution was rapidly stirred at 50 °C for 180 min, and adding acetic acid to keep the solution at pH of 4. Then, the reaction products were repeatedly washed by decompression filtration. Finally, the reaction products were desiccated and milled at a size of 200 mesh. To avoid the effect of the particle size of LDH, the particle size of unmodified LDH was also 0.075 mm.

### 2.3. X-ray photoelectron spectroscopy (XPS) test

The surface chemical properties (the composition and chemical state of element) of OLDH and LDH were acquired by XPS (Thermo Fisher Scientific Co., Ltd, USA) with Al target K<sub>α</sub> X-ray (1486.6 eV) at the vacuum of 10<sup>−9</sup> Pa.

**Table 1** The main performance parameters of bitumen and SBS

Samples	Items	Values
Bitumen	Penetration (25 °C, 0.1 mm)	69.0
	Ductility (10 °C, cm)	16.2
	Softening point (°C)	50.1
	Viscosity (135 °C, Pa s)	0.49
SBS	Structure	Linear
	Block ratio (S/B)	30/70
	The average molecular weight (g mol <sup>−1</sup> )	100 000

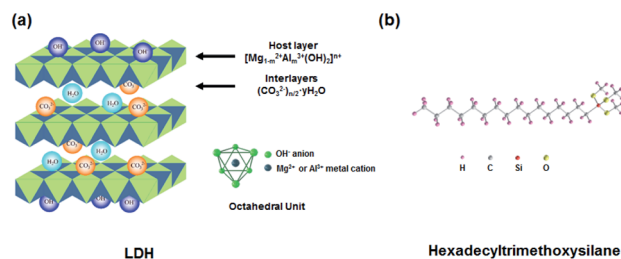


**Fig. 1** (a) The structural diagram of LDH and (b) the structural formula of hexadecyltrimethoxysilane.

### 2.4. Contact angle meter (CAM) test

The surface hydrophilia properties of OLDH and LDH were obtained by CAM (Pellet Method, KRUSS, GER) at a water droplet volume of 2 μL and a dropping speed of 1 μL s<sup>−1</sup>.

### 2.5. Preparation of OLDH/SBS modified bitumen

Firstly, bitumen samples were melted to be flowable at 170 ± 5 °C. Subsequently, 3.5% SBS was dispersed into flowing binder samples under the high-speed shearing, and the mixture was sheared at 180 °C for 60 min. Then, 1% to 4% LDH or OLDH were slowly appended to the binder samples. Finally, the mixture continued to react at the mechanical agitation for 90 min. To facilitate later description, SMB containing OLDH and OLDH were abbreviated as LSMB and OLSMB, respectively.

### 2.6. Aging of SMB

Firstly, SMB was placed in thin film oven at 163 ± 0.5 °C for 5 h, with the purpose to imitate the short-term thermal oxygen aging of SMB during the preparing and paving process. Then, to simulate the UV aging of SMB during the service, the vestigial binder samples were shifted to an UV aging oven at 60 ± 3 °C for 9 d.

### 2.7. Physical and rheological properties test

The dispersibility and stability is crucial to the anti-aging ability of SMB. To assess this, the storage stability of all SMB samples was conducted. Firstly, the flowing samples was poured into Al pipe, and putting the pipe into an oven at 163 ± 5 °C for 2 d. Whereafter, these samples were transferred to a cooler for 210 min. Finally, the pipe was equally cut into three parts. The softening points of top and bottom part were tested, the softening point difference (ΔS) of two parts were utilized to estimate the stability of LDH in SMB.

The conventional physical properties (penetration, softening point and ductility) tests of all binder samples were according to ASTM D 5, D 36 and D 113. The viscosity was measured based on D 4402.

The dynamic rheological properties of all SMB samples were obtained by dynamic shear rheometer (DSR, Anton Paar Corp., AUT). The measuring parameters are listed in Table 2.

### 2.8. Fourier transform infrared spectroscopy (FTIR) test

The chemical structure of all SMB samples was gained by FTIR (Thermo Nicolet Corp., USA). The test wavenumber was from

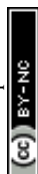


Table 2 The measuring parameters of rheological properties for SMB

Measuring temperature (°C)	Diameter of plate (mm)	Gap between plates (mm)	Sweep frequency (rad s <sup>-1</sup> )	Heating rate (°C min <sup>-1</sup> )
−10 to 30	8	2	10	2
30 to 80	25	1	10	2

400 cm<sup>-1</sup> to 4000 cm<sup>-1</sup>. The relevant scanning rate and resolution were 64 min<sup>-1</sup> and 4 cm<sup>-1</sup>.

### 3. Results and discussion

#### 3.1. XPS analysis of OLDH

The wide survey spectra of XPS for LDH and OLDH are depicted in Fig. 2. It can be found that some characteristic elements were appeared in the XPS of LDH and OLDH, like Mg 1s at 1302.5 eV, Mg 2s at 88.9 eV and Al 2p at 74.1 eV. The Mg and Al element was belonged to the metallic-oxide laminate in LDH.<sup>26,27</sup> In addition, compared with LDH, it was noteworthy that a new element (Si 2p at 103.1 eV) can be observed in the XPS of OLDH, which was attributed to hexadecyltrimethoxysilane. The results showed that hexadecyltrimethoxysilane has been connected with LDH, but it could not confirm that the connection was chemical bond combination or physical entanglement of molecular chains.

To affirm the connection type between hexadecyltrimethoxysilane and LDH. The high energy resolution spectra of Si 2p (103.1 eV) for OLDH is presented in Fig. 3. Three peaks (102.5, 103.6 and 104.0 eV) can be observed, the peak at 102.5 eV was belonged to Si–C, and the peak at 103.6 eV was attributed to Si–O–C,<sup>27,28</sup> the two peaks were derived from hexadecyltrimethoxysilane. The peak at 104.0 eV was originated from Si–O–M (M = Al or Mg), the Si–O–M was newly generated chemical bond, which can not be found in hexadecyltrimethoxysilane and LDH. The result indicated that hexadecyltrimethoxysilane has been chemically bonded to LDH. The related chemical reaction paths between hexadecyltrimethoxysilane and LDH are shown in

Fig. 4. Firstly, the hexadecyltrimethoxysilane hydrolyzed to produce Si–OH. Then, the Si–OH reacted with the surface –OH of LDH and generated Si–O–M. Finally, hexadecyltrimethoxysilane was chemically grafted onto LDH.

#### 3.2. Hydrophilicity analysis of OLDH

The water contact angles of LDH and OLDH are depicted in Fig. 5. The contact angle of LDH was 19.1°, it indicated that LDH possessed excellent hydrophilicity, which was due to the surface –OH of LDH. Compared with LDH, the contact angle of OLDH significantly increased to 97.1°, it showed that the surface of LDH transformed from hydrophilia to lipophilicity after hexadecyltrimethoxysilane organic modification.

Hexadecyltrimethoxysilane organic modification reduced the surface –OH (polar group) of LDH, the decrease of polar groups was conducive to ameliorate the dispersibility of LDH in SMB. Simultaneously, it will introduce organic groups in LDH after hexadecyltrimethoxysilane organic modification, which can further improve the stability of LDH in SMB. The double action of hexadecyltrimethoxysilane organic modification caused the hydrophilicity of LDH decrease, which will contribute to strengthen the dispersibility and stability of LDH in hydrophobic SMB matrix.

#### 3.3. Storage stability

The storage stability of all SMB samples is portrayed in Fig. 6. The ΔS of SMB was 2.4 °C, it showed that SBS has occurred isolation in bitumen. SBS will assimilate the light constituent (saturate or aromatic) of bitumen and swell, which resulted in

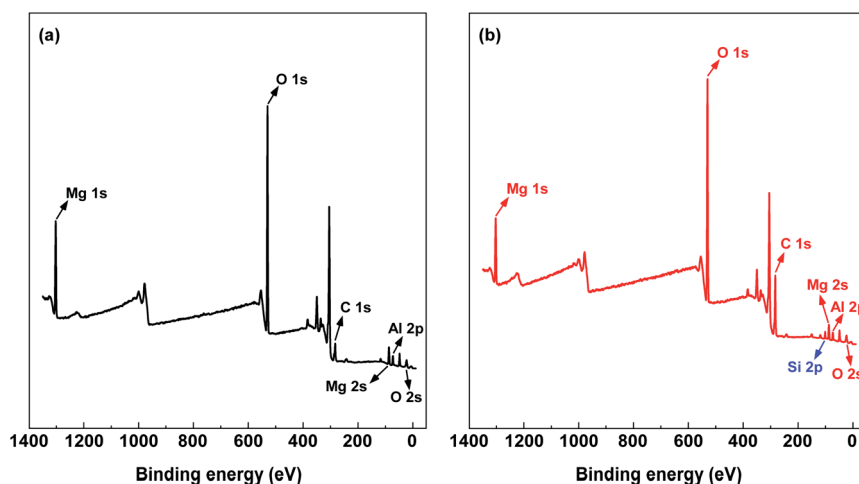


Fig. 2 The wide survey spectra of XPS: (a) LDH and (b) OLDH.



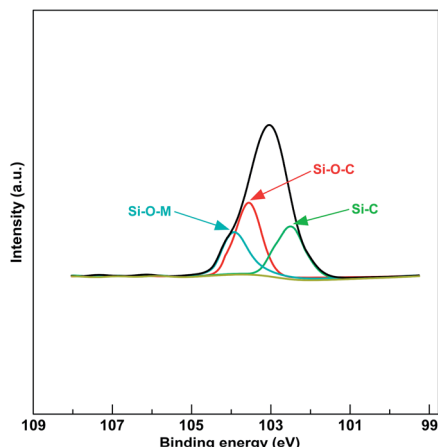


Fig. 3 The high energy resolution spectra of XPS for Si 2p.

the floating of SBS in bitumen, and induced the softening point of the upper increase. Compared with SMB, the  $\Delta S$  of LSMB obviously decreased. Furthermore, the downtrend became more apparent with the dosage of LDH increase. However, it was noteworthy that the lesser  $\Delta S$  of LSMB did not mean the better dispersibility and stability of LDH in SMB, this was due to the sedimentation of LDH in bitumen, which caused the softening point of the bottom increase. Because of the opposite effect of LDH and SBS on the softening point of SMB during the storage stability test, it eventually led to the rapid decrease of  $\Delta S$  with the amount of LDH increase. Similarly to LSMB, the  $\Delta S$  of OLSMB decreased with the content of LDH increase, but the downtrend was distinctly weakened. The cause of this situation was that hexadecyltrimethoxysilane organic modification relieved the agglomeration of LDH and improved the dispersibility and stability of LDH in SMB. The result showed that

OLDH exhibited better dispersibility and stability in SMB compared with LDH.

### 3.4. Physical properties

The physical properties of all SMB samples with different dosage of OLDH and LDH are plotted in Fig. 7. Compared with SMB, it can be observed that OLSMB and LSMB had smaller penetration and ductility, larger soften point and viscosity. Furthermore, this tendency became more prominent with the dosage of OLDH and LDH increase. The reason for this is that LDH is inorganic particles, the addition of LDH in SMB serves as elastic component, and will impede the movement of SBS and bitumen molecule to a certain extent. Moreover, compared with LDH, it was also noteworthy that OLDH showed more significant impact on the penetration, soften point and viscosity of SMB, because of the better dispersibility and stability of OLDH in SMB.

After aging, the penetration and ductility of SMB remarkably diminished, correspondingly, the soften point and viscosity obviously enlarged. To estimate the physical performance change of SMB before and after aging, the aging indexes of physical performances (PRR, SPI, DRR and VAI) were utilized in this research, the larger the PRR and DRR, the smaller the SPI and VAI, the better anti-aging performance of SMB.<sup>29</sup> The computational formulas of these aging indexes are as follows (1)–(4):

$$\text{PRR} = \frac{(\text{penetration after aging})}{(\text{penetration before aging})} \times 100 \quad (1)$$

$$\text{SPI} = \frac{(\text{softening point after aging} - \text{softening point before aging})}{\text{softening point before aging}} \quad (2)$$

$$\text{DRR} = \frac{(\text{ductility after aging})}{(\text{ductility before aging})} \times 100 \quad (3)$$

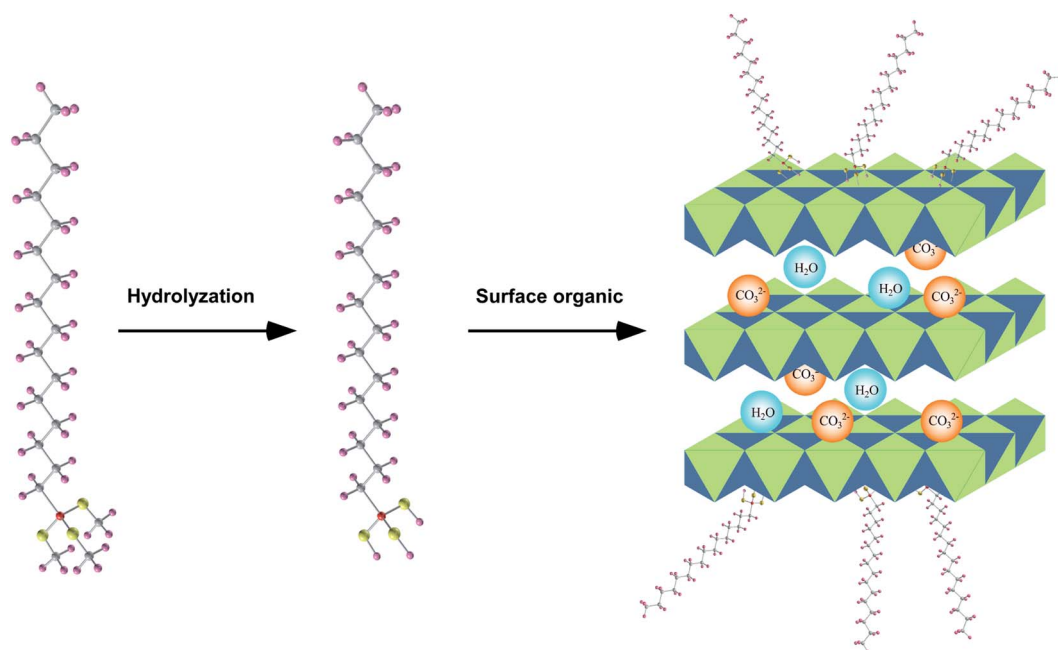


Fig. 4 The chemical reaction process between hexadecyltrimethoxysilane and LDH.



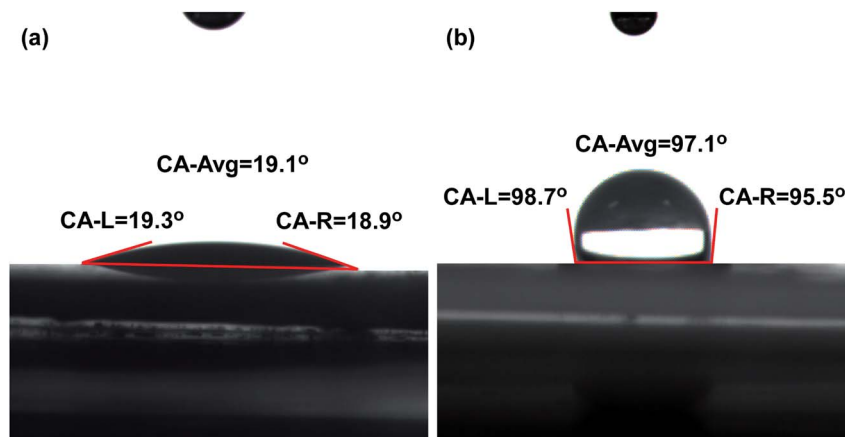


Fig. 5 The water contact angles of (a) LDH and (b) OLDH.

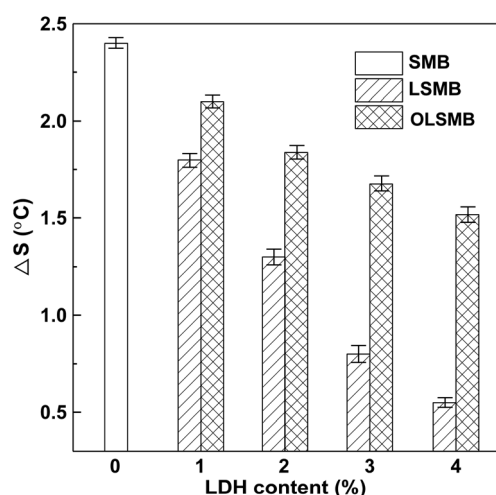


Fig. 6 The storage stability of all SMB samples.

$$\text{VAI} = \frac{(\text{viscosity after aging} - \text{viscosity before aging})}{\text{viscosity before aging}} \times 100 \quad (4)$$

The aging indexes of all SMB samples containing OLDH and LDH are depicted in Fig. 7. Compared with SMB, the PRR and DRR of OLSMB and LSMB were larger, the SPI and VAI were smaller, and the tendency became more obvious with the content of LDH increase. It indicated that OLDH or LDH can alleviate the destruction of aging on the physical performances of SMB, and the alleviation effect became more prominent with LDH content increase. Additionally, it can be found that OLDH exhibited better in inhibiting the physical properties deterioration of SMB than that of LDH during aging.

### 3.5. Rheological properties

The elasticity modulus ( $G'$ ) and viscous modulus ( $G''$ ) of all SMB specimens from  $-10^\circ\text{C}$  to  $30^\circ\text{C}$  are depicted in Fig. 8. The  $G'$  and  $G''$  of all SMB specimens decreased with the temperature increase, and the descending rate of  $G'$  were apparently higher than that of  $G''$ . An intersection point between  $G'$  and  $G''$  can be

observed in all SMB specimens,  $G'$  was larger than  $G''$  before the corresponding temperature of intersection point, in other words, SMB showed more elastic behavior before the temperature. After the corresponding temperature of intersection point,  $G''$  gradually became greater than  $G'$ , SMB exhibited more viscous behavior. It showed that the corresponding temperature of the intersection point was the critical temperature of visco-elastic transformation for SMB. Compared with SMB, LSMB and OLSMB possessed larger  $G'$  and smaller  $G''$  at the same temperature, which indicated that LDH and OLDH can increase  $G'$  of SMB and reduce  $G''$ . Meanwhile, the corresponding temperature of the intersection point was also increased. This variation was detrimental to the low temperature properties of SMB, fortunately, due to the less dosage, the effect of LDH and OLDH was little.

The  $G'$  and  $G''$  of all SMB specimens after aging are plotted in Fig. 9. After aging, the  $G'$  of all SMB samples increased in different extent,  $G''$  simultaneously reduced. The variation of SMB was the most obvious, followed by LSMB, OLSMB was the least. The size order of  $G'$  and  $G''$  of SMB, LSMB and OLSMB was the opposite of that before aging. Correspondingly, the corresponding temperature of the intersection point of SMB, LSMB and OLSMB before and after aging also occurred different changes. As showed in Table 3, the corresponding temperature of the intersection point of SMB increased to  $27.2^\circ\text{C}$  after aging, the increment of temperature ( $\Delta T$ ) was  $11.6^\circ\text{C}$ . The addition of LDH and OLDH obviously retarded the corresponding temperature change of the intersection point of SMB, the  $\Delta T$  of LSMB was  $6.3^\circ\text{C}$ , the  $\Delta T$  of OLSMB was  $0.9^\circ\text{C}$ . The result showed that the aging led to the elastic behavior increase of SMB, the corresponding temperature of the intersection point enlarged, these were not conducive to the low temperature performance of SMB. LDH can alleviate the destruction of aging on the low temperature performance of SMB. Furthermore, the alleviation effective of LDH was remarkably strengthened after hexadecyltrimethoxysilane organic modification.

The rutting factor ( $G^*/\sin \delta$ ) reflects the resistance capacity of bitumen to permanent deformation at high temperature, the larger the  $G^*/\sin \delta$ , the better the high temperature stability.



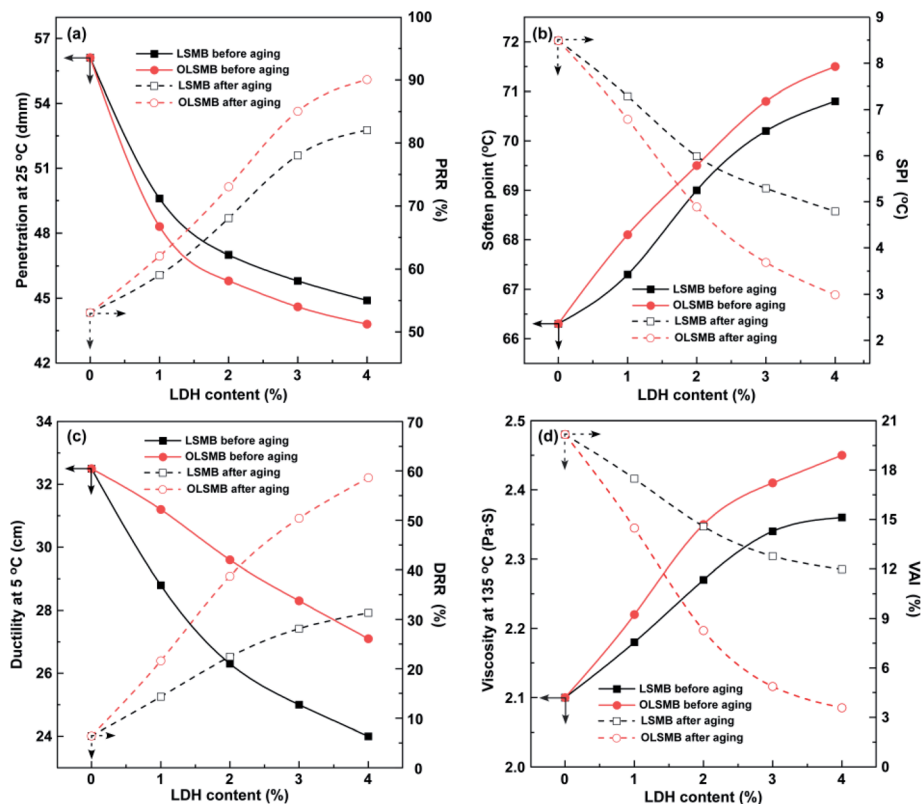


Fig. 7 The physical properties of all SMB samples before and after aging: (a) penetration; (b) soften point; (c) ductility; (d) viscosity.

The  $G^*/\sin \delta$  of all SMB specimens ranging from 30 °C to 80 °C are illustrated in Fig. 10. The  $G^*/\sin \delta$  of LSMB and OLSMB were greater than that of SMB, it indicated that the addition of LDH and OLDH can ameliorate the high-temperature stability of SMB, particularly OLDH. After aging, the  $G^*/\sin \delta$  of all SMB samples increased to a different extent, SMB showed the most significant, OLSMB was the least. The size order of  $G^*/\sin \delta$  was SMB > LSMB > OLSMB after aging, which was exactly opposite with that before aging. The rapid increase of  $G^*/\sin \delta$  did not mean the high-temperature stability improvement of SMB. On

the contrary, due to the aging, SMB became hard and brittle, the performance of SMB was deteriorated. The introduction of OLDH and LDH can inhibit the performance deterioration of SMB, and improve the anti-aging capacity of SMB, especially OLDH.

### 3.6. Chemical structure

The FTIR spectrum of all SMB samples are presented in Fig. 11. Compared with SMB, an obvious absorption peak located at

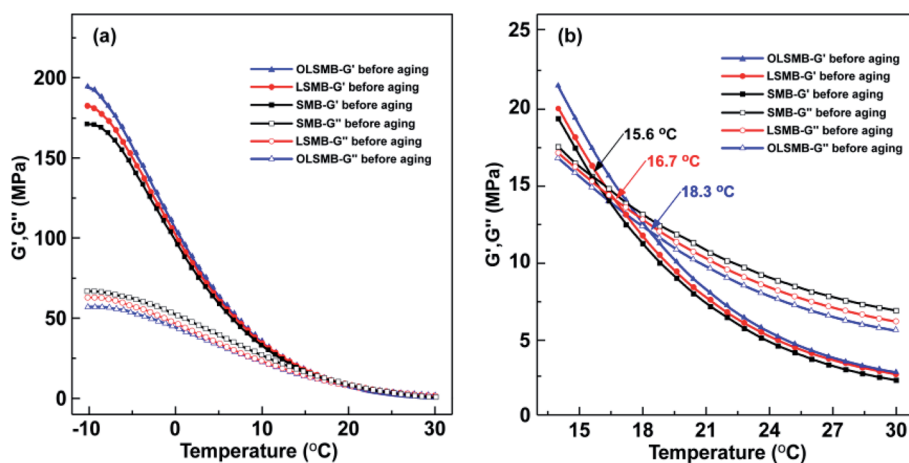
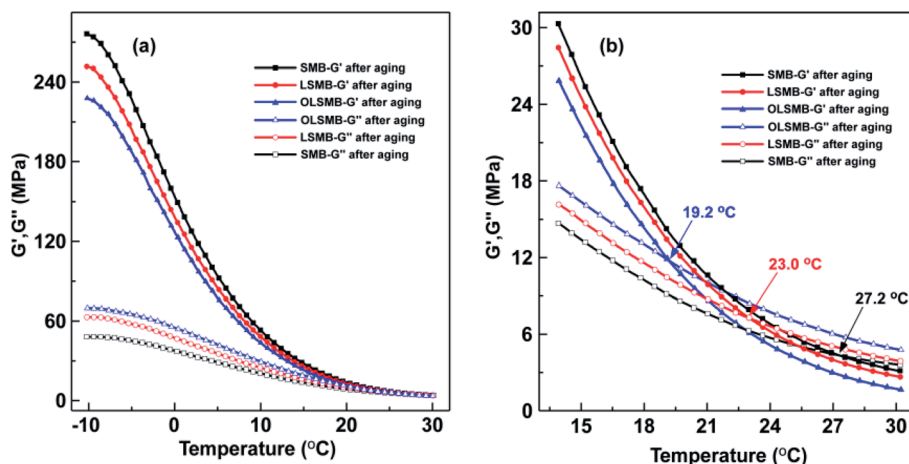
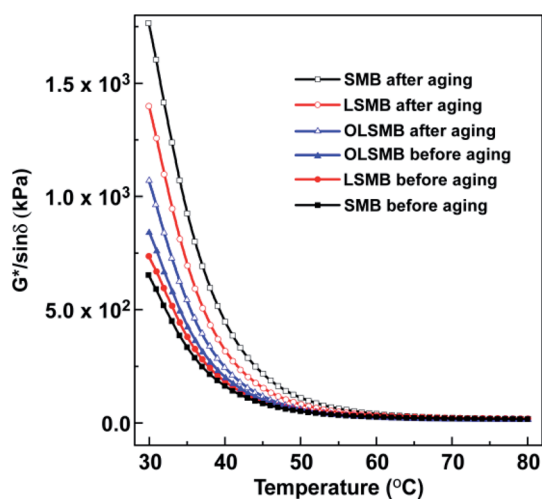


Fig. 8  $G'$  (a) and  $G''$  (b) of all SMB samples before aging.



Fig. 9  $G'$  (a) and  $G''$  (b) of all SMB samples after aging.Table 3 The temperature of intersection point of all SMB samples<sup>a</sup>

Samples	The temperature of intersection point (°C)		$\Delta T$ (°C)
	Before aging	After aging	
SMB	15.6	27.2	11.6
LSMB	16.7	23.0	6.3
OLSMB	18.3	19.2	0.9

<sup>a</sup>  $\Delta T$  = The temperature after aging – the temperature before aging.Fig. 10  $G^*/\sin \delta$  of all SMBpa samples before and after aging.

$3450\text{ cm}^{-1}$  can be observed in the FTIR spectrum of LSMB and OLSMB, belonging to the interstratified crystallization water of LDH and OLDH. Additionally, in the LDH and OLDH, some absorption peaks were appeared in the lower wavenumber, for instance,  $545\text{ cm}^{-1}$ ,  $451\text{ cm}^{-1}$ , these peaks were ascribed to the lattice vibration of metallic-oxide laminate of LDH and OLDH.

The aging of SMB was complex chemical reactions, which contained the oxidation of bitumen and degradation of SBS. To estimate the chemical structure variation of SMB before and after aging, some characteristic functional groups were utilized, such as the  $\text{C}=\text{O}$  and  $\text{S}=\text{O}$  for bitumen,  $\text{C}=\text{C}$  for SBS.<sup>30,31</sup> The calculating methods are listed as formulas (5)–(8):

$$I_{\text{C}=\text{O}} = \frac{\text{Area of carbonyl band centered around } 1700\text{ cm}^{-1}}{\sum \text{area of spectral bands between } 2000\text{ cm}^{-1} \text{ and } 600\text{ cm}^{-1} \times 100} \quad (5)$$

$$I_{\text{S}=\text{O}} = \frac{\text{Area of carbonyl band centered around } 1030\text{ cm}^{-1}}{\sum \text{area of spectral bands between } 2000\text{ cm}^{-1} \text{ and } 600\text{ cm}^{-1} \times 100} \quad (6)$$

$$I_{\text{C}=\text{C}} = \frac{\text{Area of carbonyl band centered around } 966\text{ cm}^{-1}}{\sum \text{area of spectral bands between } 2000\text{ cm}^{-1} \text{ and } 600\text{ cm}^{-1} \times 100} \quad (7)$$

$$v = \left| \frac{v_{\text{after aging}} - v_{\text{before aging}}}{v_{\text{before aging}}} \right| \quad (8)$$

The characteristic group content of all SMB samples is listed in Table 4. The  $\text{C}=\text{O}$ ,  $\text{S}=\text{O}$  and  $\text{C}=\text{C}$  of all SMB samples were basically identical before aging, it indicated that the introduction of LDH and OLDH would not affect the characteristic group content of SMB. After aging, the content of  $\text{C}=\text{O}$  and  $\text{S}=\text{O}$  increased, it was due to the oxidation of bitumen molecular. Correspondingly, the content of  $\text{C}=\text{C}$  reduced, because of the degradation of SBS molecular. Compared with SMB ( $v_{\text{C}=\text{O}} = 19.56$ ,  $v_{\text{S}=\text{O}} = 2.45$  and  $v_{\text{C}=\text{C}} = 0.45$ ), the addition of LDH obviously suppressed the increase of  $\text{C}=\text{O}$  and  $\text{S}=\text{O}$  ( $v_{\text{C}=\text{O}} = 16.42$  and  $v_{\text{S}=\text{O}} = 1.99$ ), and the decrease of  $\text{C}=\text{C}$  ( $v_{\text{C}=\text{C}} = 0.30$ ). Furthermore, the inhibitory effect of LDH were further



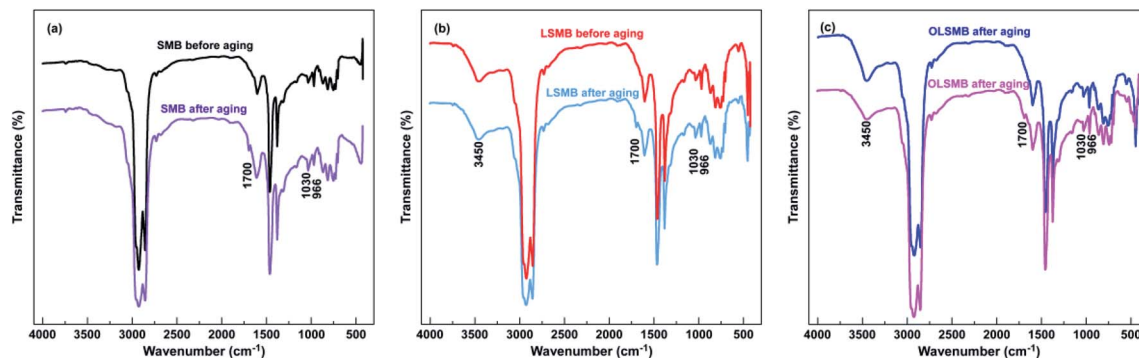


Fig. 11 FTIR spectrum of all SMB samples before and after aging: (a) SMB, (b) LSMB, (c) OLSMB.

Table 4 The characteristic groups content of all SMB samples

Bitumen samples	Before aging			After aging			Change rate		
	$I_{C=O}$	$I_{S=O}$	$I_{C=C}$	$I_{C=O}$	$I_{S=O}$	$I_{C=C}$	$v_{C=O}$	$v_{S=O}$	$v_{C=C}$
SMB	0.255	3.421	9.523	5.242	11.805	5.205	19.56	2.45	0.45
LSMB	0.253	3.382	9.518	4.408	10.118	6.644	16.42	1.99	0.30
OLSMB	0.256	3.424	9.521	2.998	7.015	7.532	10.71	1.05	0.21

enhanced after hexadecyltrimethoxysilane organic modification, the  $v_{C=O}$ ,  $v_{S=O}$  and  $v_{C=C}$  of OLSMB were 10.71, 1.05 and 0.21, respectively. The result showed that LDH can mitigate the oxidation of bitumen and degradation of SBS, inhibit the chemical structure variation of SMB, improve the anti-aging ability of SMB, and OLDH presented more excellent improvement on the anti-aging ability of SMB.

## 4. Conclusions

LDH organically modified by hexadecyltrimethoxysilane was prepared and used to enhance the anti-aging performance of SMB. According to the analysis results, the relevant research conclusions are as follows:

(1) Hexadecyltrimethoxysilane was grafted into LDH through the chemical bonds. Hexadecyltrimethoxysilane organic modification decreased the hydroxide radicals and introduced organic groups into LDH, the hydrophilicity of organic LDH was obviously reduced. The stability of LDH in SMB has been obviously improved after hexadecyltrimethoxysilane organic modification.

(2) The addition of OLDH and LDH can enhance the high temperature stability of SMB, particularly OLDH. After aging, the physical and rheological properties of SMB were badly deteriorated. LDH can alleviate the damage of aging on the performance of SMB. Furthermore, the alleviation effect of OLDH was more notable.

(3) The aging resulted in the oxidation of bitumen and the degradation of SBS. OLDH and LDH can refrain the chemical structure variation of SMB during aging, OLDH exhibited better improvement on the anti-aging ability of SMB compared with LDH.

## Conflicts of interest

There are no conflicts to declare.

## Acknowledgements

This work is supported by National Natural Science Foundation of China (52008113), Educational Research Projects for Young and Middle-Aged Teachers of Education Department of Fujian Province (JAT190047), Open Fund of Key Laboratory of Road Structure and Material of Ministry of Transport, Chang'an University (300102210509) and State Key Laboratory of Special Functional Waterproof Materials (SKLW2019012). The authors gratefully acknowledge their financial support.

## References

- 1 J. Q. Zhu, B. Birgisson and N. Kringos, *Eur. Polym. J.*, 2014, **54**, 18–38.
- 2 Y. Yidirim, *Constr. Build. Mater.*, 2007, **21**, 66–72.
- 3 G. D. Airey, *J. Mater. Sci.*, 2004, **39**, 951–959.
- 4 H. L. Zhang, Z. H. Chen, G. Q. Xu and C. Shi, *J. Fuels.*, 2018, **221**, 78–88.
- 5 S. P. Wu, L. Pang, L. T. Mo, Y. C. Chen and G. Zhu, *Constr. Build. Mater.*, 2009, **23**, 1005–1010.
- 6 X. H. Lu and U. Isacson, *Fuel*, 1998, **77**, 961–972.
- 7 Y. Y. Li, S. P. Wu, Y. Dai, C. M. Li, W. Song, H. C. Li, C. Li and B. A. Shu, *Fuel*, 2020, **262**, 116507.
- 8 F. S. Wang, J. Xie, S. P. Wu, J. S. Li, D. M. Barbieri and L. Zhang, *Renewable Sustainable Energy Rev.*, 2021, **141**, 110823.



- 9 Z. G. Feng, J. Y. Yu, L. H. Xue and Y. B. Sun, *J. Appl. Polym. Sci.*, 2013, **128**, 2571–2577.
- 10 P. L. Cong, X. Wang, P. J. Xu, J. F. Liu, R. He and S. F. Chen, *Polym. Degrad. Stab.*, 2013, **98**, 2627–2634.
- 11 D. M. Zhang, Z. H. Chen, H. L. Zhang and C. W. Wei, *Constr. Build. Mater.*, 2018, **188**, 409–416.
- 12 Z. G. Feng, J. Y. Yu and D. L. Kuang, *Pet. Sci. Technol.*, 2013, **31**, 113–120.
- 13 X. L. Zou, A. M. Sha, B. A. Ding, Y. Q. Tan and X. N. Huang, *Adv. Mater. Sci. Eng.*, 2017, 6319697.
- 14 S. Filippi, M. Cappello, M. Merce and G. Polacco, *J. Nanomater.*, 2018, 2469307.
- 15 L. Guo, W. Wu, Y. F. Zhou, F. Zhang, R. C. Zeng and J. M. Zeng, *J. Mater. Sci. Technol.*, 2018, **34**, 1455–1466.
- 16 S. Mallakpour, M. Hatami and C. M. Hussain, *Adv. Colloid Interface Sci.*, 2020, **283**, 102216.
- 17 Q. Wang and D. O'Hare, *Chem. Rev.*, 2017, **2633**, 147–153.
- 18 C. L. Zhang, J. Y. Yu, X. Xu and Y. B. Sun, *Pet. Sci. Technol.*, 2017, **35**, 488–494.
- 19 Y. Y. Li, S. P. Wu, L. Pang, Q. T. Liu, Z. F. Wang and A. M. Zhang, *Constr. Build. Mater.*, 2018, **172**, 584–596.
- 20 C. Peng, G. S. Jiang, C. H. Lu, F. Xu, J. Y. Yu and J. Dai, *RSC Adv.*, 2015, **5**, 95504–95511.
- 21 C. L. Zhang, J. Y. Yu, K. Feng, L. H. Xue and D. Xie, *Appl. Clay Sci.*, 2016, **120**, 1–8.
- 22 B. Y. He, J. Y. Yu, Y. Gu, R. H. Zhuang and Y. B. Sun, *Constr. Build. Mater.*, 2018, **180**, 342–350.
- 23 S. Xu, J. Y. Yu, C. L. Zhang, T. T. Yao and Y. B. Sun, *Mater. Struct.*, 2016, **49**, 1235–1244.
- 24 C. Peng, J. Dai, J. Y. Yu and J. Yin, *AIP Adv.*, 2015, **5**, 027133.
- 25 S. Kango, S. Kalia, A. Celli, J. Njuguna, Y. Habibi and R. Kumar, *Prog. Polym. Sci.*, 2013, **38**, 1232–1261.
- 26 C. L. Zhang, T. Wang, M. Yu, S. Xu, Z. G. Feng, C. B. Hu and W. F. Duan, *Constr. Build. Mater.*, 2021, **292**, 123411.
- 27 W. Z. Xu, S. Q. Wang, A. J. Li and X. L. Wang, *RSC Adv.*, 2016, **6**, 48189–48198.
- 28 J. L. Jiang, Y. B. Wang, J. F. Du, H. Yang and J. Y. Hao, *Appl. Surf. Sci.*, 2016, **379**, 516–522.
- 29 C. Z. Zhu, H. L. Zhang, D. M. Zhang and Z. H. Chen, *J. Mater. Civ. Eng.*, 2018, **30**, 04017306.
- 30 C. Q. Yan, W. D. Huang, F. P. Xiao, L. F. Wang and Y. W. Li, *Road Mater. Pavement Des.*, 2018, **19**, 1406–1421.
- 31 Y. T. Li, L. F. Li, Y. Zhang, S. F. Zhao, L. D. Xie and S. D. J. Yao, *Appl. Polym. Sci.*, 2010, **116**, 754–761.

